



**HAL**  
open science

## A new empirical model for radar scattering from bare soil surfaces

N. Baghdadi, M. Choker, Mehrez Zribi, Mohammad El Hajj, S. Paloscia, N.E.C. Verhoest, H. Lievens, Frédéric Baup, F. Mattia

### ► To cite this version:

N. Baghdadi, M. Choker, Mehrez Zribi, Mohammad El Hajj, S. Paloscia, et al.. A new empirical model for radar scattering from bare soil surfaces. *Reviews on Advanced Materials Science*, 2016, 8 (11), pp.920. 10.3390/rs8110920 . hal-01529350

**HAL Id: hal-01529350**

**<https://hal.science/hal-01529350>**

Submitted on 30 May 2017

**HAL** is a multi-disciplinary open access archive for the deposit and dissemination of scientific research documents, whether they are published or not. The documents may come from teaching and research institutions in France or abroad, or from public or private research centers.

L'archive ouverte pluridisciplinaire **HAL**, est destinée au dépôt et à la diffusion de documents scientifiques de niveau recherche, publiés ou non, émanant des établissements d'enseignement et de recherche français ou étrangers, des laboratoires publics ou privés.

1 Article

# 2 A New Empirical Model for Radar Scattering from 3 Bare Soil Surfaces

4 Nicolas Baghdadi<sup>1</sup>, Mohammad Choker<sup>1</sup>, Mehrez Zribi<sup>2</sup>, Mohammad El Hajj<sup>1</sup>, Simonetta  
5 Paloscia<sup>3</sup>, Niko E.C. Verhoest<sup>4</sup>, Hans Lievens<sup>4,5</sup>, Frederic Baup<sup>2</sup>, Francesco Mattia<sup>6</sup>

6 <sup>1</sup> IRSTEA, UMR TETIS, 500 rue François Breton, F-34093 Montpellier cedex 5, France ;  
7 E-Mails : nicolas.baghdadi@teledetection.fr; mohammad.choker@teledetection.fr;  
8 mohammad.el-hajj@teledetection.fr

9 <sup>2</sup> CESBIO, 18 av. Edouard Belin, bpi 2801, 31401 Toulouse cedex 9, France;  
10 E-Mails: mehrez.zribi@ird.fr; frederic.baup@cesbio.cnes.fr

11 <sup>3</sup> CNR-IFAC, via Madonna del Piano 10, 50019 Sesto Fiorentino, Firenze, Italy;  
12 E-Mail: s.paloscia@ifac.cnr.it

13 <sup>4</sup> Laboratory of Hydrology and Water Management, Ghent University, Ghent B-9000, Belgium;  
14 E-Mails: niko.verhoest@UGent.be ; hans.lievens@UGent.be

15 <sup>5</sup> Global Modeling and Assimilation Office, NASA Goddard Space Flight Center, Greenbelt, MD 20771 USA;  
16 E-Mails: Hans.Lievens@UGent.be (H.L.)

17 <sup>6</sup> CNR-ISSIA, via Amendola 122/D, Bari 70126, Italy; E-Mail: mattia@ba.issia.cnr.it

18 **Abstract:** The objective of this paper is to propose a new semi-empirical radar backscattering  
19 model for bare soil surfaces based on the Dubois model. A wide dataset of backscattering  
20 coefficients extracted from SAR (synthetic aperture radar) images and in situ soil surface parameter  
21 measurements (moisture content and roughness) is used. The retrieval of soil parameters from SAR  
22 images remains challenging because the available backscattering models have limited  
23 performances. Existing models, physical, semi-empirical or empirical, do not allow for a reliable  
24 estimate of soil surface geophysical parameters for all surface conditions. The proposed model,  
25 developed in HH, HV and VV polarizations, uses a formulation of radar signals based on physical  
26 principles that validated in numerous studies. Never before has a backscattering model been built  
27 and validated on such an important dataset as the one proposed in this study. It contains a wide  
28 range of incidence angles (18°-57°) and radar wavelengths (L, C, X), well distributed geographically  
29 for regions with different climate conditions (humid, semi-arid and arid sites) and involving many  
30 SAR sensors. The results show that the new model shows a very good performance for different  
31 radar wavelength (L, C, X), incidence angles, and polarizations (RMSE about 2 dB). This model is  
32 easy to invert and could provide a way to improve the retrieval of soil parameters.

33 **Keywords:** New backscattering model, Dubois model, SAR images, Soil parameters.  
34

## 35 1. Introduction

36 Soil moisture content and surface roughness play an important roles in meteorology,  
37 hydrology, agronomy, agriculture, and risk assessment. These soil surface characteristics can be  
38 estimated using synthetic aperture radar (SAR). Today, several high-resolution SAR images can be  
39 acquired on a given study site with the availability of SAR data in L-band (ALOS-2), C-band (Sentinel-1),  
40 and X-band (TerraSAR-X, COSMO-SkyMed). In addition, it is possible to obtain SAR and optical  
41 data for global areas at high spatial and temporal resolutions with free and open access Sentinel-1/2  
42 satellites (6 days with the two Sentinel-1 and 5 days with the two Sentinel-2 satellites at 10 m spatial  
43 resolution). This availability of both Sentinel-1 satellites and Sentinel-2 sensors in addition to  
44 Landsat-8 (also free and open access) allows the combination of SAR and optical data to estimate soil  
45 moisture and vegetation parameters in operational mode.

46 The retrieval of soil moisture content and surface roughness requires the use of radar  
47 backscatter models capable of correctly modeling the radar signal for a wide range of soil parameter  
48 values. This estimation from imaging radar data implies the use of backscattering electromagnetic  
49 models, which can be physical, semi-empirical or empirical. The physical models (e.g., Integral  
50 Equation Model "IEM," Small Perturbation Model "SPM," Geometrical Optic Model "GOM,"  
51 Physical Optic Model "POM," etc.) based on physical approximations corresponding to a range of  
52 surface conditions (moisture and roughness) provide site-independent relationships but have  
53 limited validity depending upon the soil roughness. As for semi-empirical or empirical models, they  
54 are often difficult to apply to sites other than those on which they were developed and are generally  
55 valid only for specific soil conditions. The empirical models are often favored by users because the  
56 models are easier to implement and invert [1–7].

57 Among the numerous semi-empirical models reported in the literature, the most popular are  
58 those developed over bare soils by Oh et al. [8–11] and Dubois et al. [12]. The Oh model uses the  
59 ratios of the measured backscatter coefficients HH/VV and HV/VV to estimate volumetric soil  
60 moisture ( $mv$ ) and surface roughness ( $Hrms$ ), while the Dubois model links the backscatter  
61 coefficients in HH and VV polarizations to the soil's dielectric constant and surface roughness.  
62 Extensive studies evaluated various semi-empirical models, but mixed results have been obtained.  
63 Some studies show good agreement between measured backscatter coefficients and those predicted  
64 by the models, while others have found great discrepancies between them (e.g., [13–16]). The  
65 discrepancy between simulations and measurements often reaches several decibels, making soil  
66 parameter estimates unusefull.

67 The objective of this paper is to propose a robust, empirical, radar backscattering model based  
68 on the Dubois model. First, the performance of the Dubois model is analyzed using a large dataset  
69 acquired at several worldwide study sites by numerous SAR sensors. The dataset consists of SAR  
70 data (multi-angular and multi-frequency) and measurements of soil moisture and surface roughness  
71 over bare soils. Then, the different terms of Dubois equations that describe the dependence between  
72 the SAR signal and both sensor and soil parameters have been validated or modified to improve the  
73 modelling of the radar signal. Ultimately, a new semi-empirical backscattering model has been  
74 developed for radar scattering in the HH, VV, and HV polarization from bare soil surfaces.

75 After a description of the dataset in section 2, section 3 describes and analyzes the potential and  
76 the limitations of the Dubois model in radar signal simulations over bare soils. In section 4, the new  
77 model is described and its performance is evaluated for different available SAR data (L-, C- and  
78 X-bands, incidence angles between 20° and 45°). Conclusions are presented in section 5.

## 79 2. Dataset description

80 A wide experimental dataset was used, consisting of SAR images and ground measurements of  
81 soil moisture content and roughness collected over bare soils at several agricultural study sites  
82 (Table 1). SAR images were acquired by various airborne and spaceborne sensors (AIRSAR, SIR-C,  
83 JERS-1, PALSAR-1, ESAR, ERS, RADARSAT, ASAR, TerraSAR-X). The radar data were available in  
84 L-, C- and X-bands (approximately 1.25 GHz, 5.3 GHz and 9.6 GHz, respectively); with incidence  
85 angles between 18° and 57°; and in HH, VV and HV polarizations. For several reference plots, the  
86 mean backscatter coefficients have been obtained from radiometrically and geometrically calibrated  
87 SAR images by averaging backscatter coefficient values for each plot for all pixels within the plot.

88  
89  
90  
91  
92  
93  
94

95  
96**Table 1.** Description of the dataset used in this study. "Fr": France, "It": Italy, "Ge": Germany, "Be": Belgium, "Lu": Luxembourg, "Ca": Canada, "Tu": Tunisia.

Site	SAR sensor	Freq	Year	Number of data
Orgeval (Fr) [17]	SIR-C	L	1994	➤ <b>HH : 1569 measurements</b> – 144 in L-band – 997 in C-band – 428 in X-band  ➤ <b>VV : 930 measurements</b> – 71 in L-band – 640 in C-band – 219 in X-band  ➤ <b>HV : 605 measurements</b> – 7 in L-band – 538 in C-band – 60 in X-band
Orgeval (Fr) [17–19]	SIR-C, ERS, ASAR	C	1994; 1995; 2008; 2009; 2010	
Orgeval (Fr) [19]	PALSAR-1	L	2009	
Orgeval (Fr) [20]	TerraSAR-X	X	2008, 2009, 2010	
Pays de Caux (Fr) [21–22]	ERS; RADARSAT	C	1998; 1999	
Villamblain (Fr) [23–25]	ASAR	C	2003; 2004;	
Villamblain (Fr) [19,26]	TerraSAR-X	X	2006 2008; 2009	
Thau (Fr) [27]	RADARSAT TerraSAR-X	C X	2010; 2011 2010	
Touch (Fr) [23,28]	ERS-2; ASAR	C	2004; 2006; 2007	
Mauzac (Fr) [26]	TerraSAR-X	X	2009	
Garons (Fr) [26]	TerraSAR-X	X	2009	
Kairouan (Tu) [29]	ASAR	C	2012	
Kairouan (Tu) [26,29, 30]	TerraSAR-X	X	2010; 2012; 2013; 2014	
Yzerons (Fr) [31]	TerraSAR-X	X	2009	
Versailles (Fr) [26]	TerraSAR-X	X	2010	
Seysses (Fr) [26]	TerraSAR-X	X	2010	
Chateauguay (Ca) [21]	RADARSAT	C	1999	
Brochet (Ca) [21]	RADARSAT	C	1999	
Alpilles (Fr) [21]	ERS; RADARSAT	C	1996; 1997	
Sardaigne (It) [32]	ASAR; RADARSAT	C	2008; 2009	
Saint Lys (Fr) [33]	PALSAR-1	L	2010	
Matera (It) [34]	SIR-C	L	1994	
Alzette (Lu) [35]	PALSAR-1	L	2008	
Dijle (Be) [35]	PALSAR-1	L	2008; 2009	
Zwalm (Be) [35]	PALSAR-1	L	2007	
Demmin (Ge) [35]	ESAR	L	2006	
Montespertoli (It) [36]	AIRSAR	L	1991	
Montespertoli (It) [37]	SIR-C	L; C	1994	
Montespertoli (It) [38]	JERS-1	L	1994	

97 In addition, in situ measurements of soil moisture ( $mv$ ) were available for each reference plot.  
 98 The soil water content was collected from the top 5 or 10 cm of each reference plot at several  
 99 locations using the gravimetric method and a calibrated TDR (time domain reflectometry) probe. In  
 100 practice, the soil moisture for each reference plot was assumed to be equal to the mean of all  
 101 measurements carried out on the reference plot within a few hours of the SAR overpasses. In our  
 102 experimental dataset, the soil moisture ranged from 2 to 47 vol.%.

103 The roughness was defined by the standard deviation of surface height ( $Hrms$ ) available for  
 104 each reference plot. From roughness profiles sampled for each reference plot using mainly laser or  
 105 needle profilometers (mainly 1 m and 2 m long and with 1 cm and 2 cm sampling intervals), the  
 106 mean of all experimental autocorrelation functions was calculated to estimate the  $Hrms$   
 107 measurement. However, for some in situ measurement campaigns, meshboard technique was used  
 108 for estimating the roughness parameters. In our dataset,  $Hrms$  surface height ranged from 0.2 to 9.6  
 109 cm ( $k Hrms$  ranged from 0.2 and 13.4,  $k$  was the radar wave number).

110 A total of 1569 experimental data acquisitions with radar signal, soil moisture content and  
 111 roughness were available for HH polarization, 930 for VV polarization, and 605 for HV polarization.

### 112 3. Validation and analysis of the Dubois model

#### 113 3.1. Description of the Dubois model

114 Dubois et al. [12] proposed an empirical model to model radar backscatter coefficients in HH  
 115 and VV polarizations ( $\sigma_{HH}^0$  and  $\sigma_{VV}^0$ ) for bare soil surfaces. The expressions of  $\sigma_{HH}^0$  and  $\sigma_{VV}^0$   
 116 depend on the radar wave incidence angle ( $\theta$ , in radians), the real part of the soil dielectric constant  
 117 ( $\epsilon$ ), the rms surface height of the soil ( $Hrms$ ), the radar wavelength ( $\lambda=2\pi/k$ , where  $k$  is the radar  
 118 wavenumber):

$$\sigma_{HH}^0 = 10^{-2.75} \left( \frac{\cos^{1.5} \theta}{\sin^5 \theta} \right) 10^{0.02\epsilon \tan \theta} (k Hrms \sin \theta)^{1.4} \lambda^{0.7} \quad (1)$$

$$\sigma_{VV}^0 = 10^{-2.35} \left( \frac{\cos^3 \theta}{\sin^3 \theta} \right) 10^{0.04\epsilon \tan \theta} (k Hrms \sin \theta)^{1.1} \lambda^{0.7} \quad (2)$$

119  $\sigma_{HH}^0$  and  $\sigma_{VV}^0$  are given in a linear scale.  $\lambda$  is in cm. The validity of the Dubois model is defined as  
 120 follows:  $k Hrms \leq 2.5$ ,  $mv \leq 35$  vol. %, and  $\theta \geq 30^\circ$ .

#### 121 3.2. Comparison between simulated and real data

122 The Dubois model shows an overestimation of the radar signal by 0.7 dB in HH polarization  
 123 and an underestimation of the radar signal by 0.9 dB in VV polarization for all data combined (Table  
 124 2). The results show that the overestimation in HH is of the same order for L-, C- and X-bands  
 125 (between 0.6 dB and 0.8 dB). For the L-band, a slight overestimation of approximately 0.2 dB of SAR  
 126 data is observed in VV polarization. Also in VV polarization, Dubois model based simulations  
 127 underestimate the SAR data in C- and X-bands by approximately 0.7 dB and 2.0 dB, respectively.

128 The rms error (RMSE) is approximately 3.8 dB and 2.8 dB in HH and VV, respectively (Table 2).  
 129 Analysis of the RMSE according the radar frequency band (L, C and X separately) shows in HH an  
 130 increase of the RMSE with the radar frequency (2.9 dB in L-band, 3.7 dB in C-band, and 4.1 dB in  
 131 X-band). In VV polarization, the quality of Dubois simulations (RMSE) is similar for L- and C-bands  
 132 but is less accurate in X-band (2.3 dB in L-band, 2.6 dB in C-band, and 3.2 dB in X-band).

133

134  
135**Table 2.** Comparison between the Dubois model and real data for all data and by range of  $kHrms$ , soil moisture ( $mv$ ) and incidence angle ( $\theta$ ). Bias = real data – model.

	Dubois for HH		Dubois for VV	
	Bias (dB)	RMSE (dB)	Bias (dB)	RMSE (dB)
<i>For all data</i>	-0.7	3.8	+0.9	2.8
<i>L-band</i>	-0.8	2.9	-0.2	2.3
<i>C-band</i>	-0.6	3.7	+0.7	2.6
<i>X-band</i>	-0.7	4.1	+2.0	3.2
<i>kHrms &lt; 2.5</i>	+0.4	3.4	+1.3	2.9
<i>kHrms &gt; 2.5</i>	-2.7	4.5	-0.1	2.5
<i>mv &lt; 20 vol. %</i>	-2.0	4.3	+0.9	2.8
<i>mv &gt; 20 vol. %</i>	+0.5	3.2	+0.9	2.8
<i><math>\theta &lt; 30^\circ</math></i>	-4.1	5.4	-0.6	2.9
<i><math>\theta &gt; 30^\circ</math></i>	+0.6	3.0	+1.5	2.7

136  
137  
138  
139  
140  
141  
142  
143

In addition, the agreement between Dubois model simulations and SAR data is analyzed according to soil roughness, moisture content and incidence angle (Figures 1 and 2). The results indicate a slight underestimation of the radar signal by the Dubois model in the case of  $kHrms$  lower than 2.5 (Dubois validation domain) for both HH and VV polarizations (Figures 1b, 2b; Table 2). For surfaces with a roughness  $kHrms$  greater than 2.5, an overestimation of the radar signal is obtained with the Dubois model in HH while the model works correctly in VV (Figures 1b, 2b; Table 2). Higher under- and overestimations are observed in HH than they are in VV (reach approximately 10 dB in HH).

144  
145  
146  
147  
148

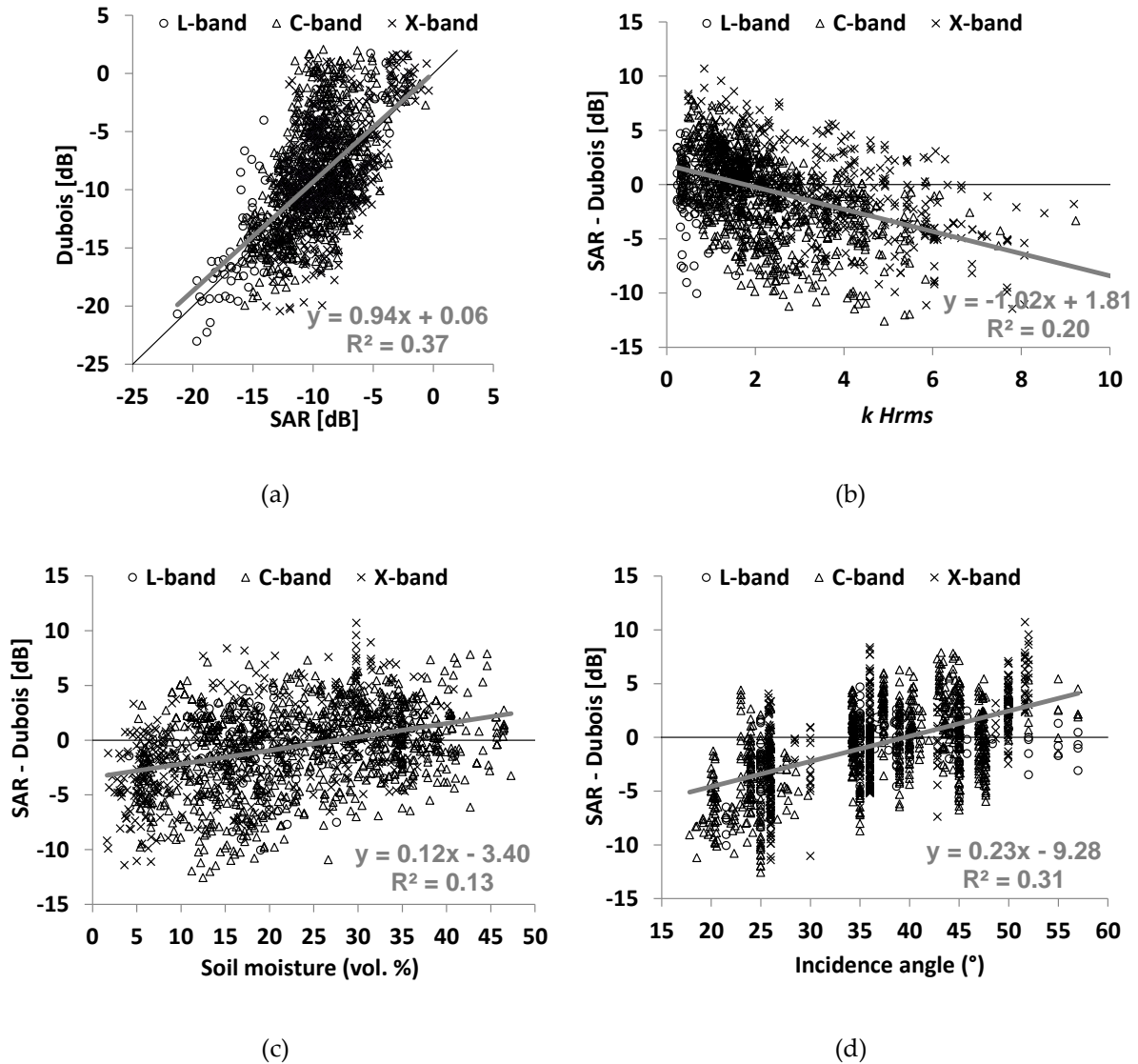
Analysis of the error as a function of soil moisture ( $mv$ ) shows that for both VV-polarized data, whatever the  $mv$ -values, and HH-polarized data with  $mv$ -values higher than 20 vol.%, the observed bias between real and simulated data is small (Figures 1c, 2c; Table 2). However, a strong overestimation of the radar signal is observed by the Dubois model in HH for  $mv$ -values lower than 20 vol.% (-2.0 dB, Table 2).

149  
150  
151  
152  
153  
154  
155

Finally, the discrepancy between SAR and the model is larger in HH for incidence angles lower than  $30^\circ$  (outside of the Dubois validity domain) than for incidence angles higher than  $30^\circ$  (Table 2). The Dubois model strongly overestimates the radar signal in HH for incidence angles lower than  $30^\circ$  but agrees closely with the measured data for incidence angles higher than  $30^\circ$  (Figures 1d, 2d; Table 2). In VV polarization, the Dubois model slightly overestimates the radar signal for incidence angles lower than  $30^\circ$  and underestimates the signal for incidence angles higher than  $30^\circ$  by +1.5 dB (Figures 1d, 2d; Table 2).

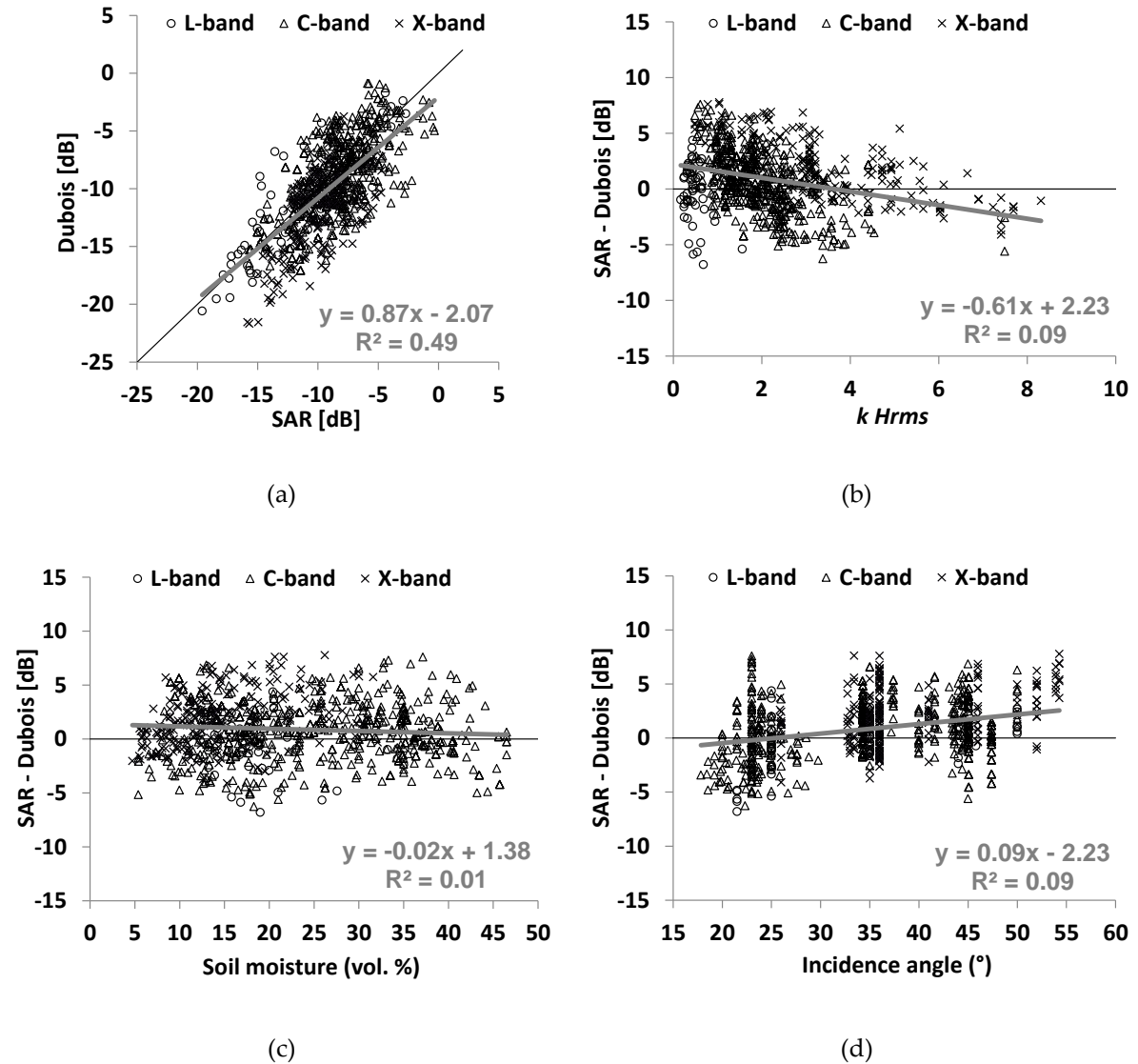
156  
157  
158

In conclusion, the Dubois model simulates VV better than it does HH (RMSE=2.8 and 3.8 dB, respectively). The disagreements observed between the Dubois model and measured data are not limited to data that are outside the optimal application domain of the Dubois model.



159 **Figure 1.** For HH polarization, (a) comparison between radar backscattering coefficients calculated  
 160 from SAR images and estimated from the Dubois model, (b) difference between the SAR signal and  
 161 the Dubois model relative to soil roughness (*kHrms*), (c) difference between the SAR signal and the  
 162 Dubois model relative to soil moisture (*mv*), (d) difference between the SAR signal and the Dubois  
 163 model relative to incidence angle. The best regression model is plotted in gray.

164



165 **Figure 2.** For VV polarization, (a) comparison between radar backscattering coefficients calculated  
 166 from SAR images and estimated from the Dubois model, (b) difference between the SAR signal and  
 167 the Dubois model relative to soil roughness ( $kHrms$ ), (c) difference between the SAR signal and the  
 168 Dubois model relative to soil moisture ( $mv$ ), (d) difference between the SAR signal and the Dubois  
 169 model relative to incidence angle. The best regression model is plotted in gray.

## 170 4. New empirical model

### 171 4.1. Methodology

172 The disagreement observed between measured and modelled radar signal encouraged us to  
 173 develop a new empirical backscattering model using SAR observations and soil in situ  
 174 measurements. The new model is based on the Dubois model and uses the dependency observed  
 175 between the SAR signal and soil parameters according to results obtained in various studies. For  
 176 bare soils, the backscattering coefficient depends on soil parameters (roughness and moisture) and  
 177 SAR instrumental parameters (incidence angle, polarization and wavelength). For bare soils, the  
 178 radar signal in pq polarization (p and q = H or V, with HV=VH) can be expressed as the product of  
 179 three components:

$$\sigma_{pq}^{\circ} = f_{pq}(\theta) g_{pq}(mv, \theta) \Gamma_{pq}(kHrms, \theta) \quad (3)$$

180 The radar backscatter coefficient is related to the incidence angle ( $\theta$ ) by the relation  $f_{pq}(\theta) =$   
 181  $\alpha(\cos \theta)^{\beta}$  ([39-41]). This relationship describes the decrease of  $\sigma^{\circ}$  with the incidence angle (decrease  
 182 higher for low angles than for high angles).

183 The second term represents the relationship between the radar backscatter coefficient and soil  
 184 moisture ( $mv$ ). The results obtained in several investigations show that, for bare soils, the radar  
 185 signal ( $\sigma^{\circ}$ ) in decibels increases linearly with soil moisture ( $mv$ ) when  $mv$  is in the range between  
 186 approximately 5 and 35 vol.% (e.g., [5,6,19,42]). In linear scale  $g_{pq}(mv, \theta)$  can be written as  
 187  $\delta 10^{\gamma mv}$ . The sensitivity of the radar signal to the soil moisture  $\gamma$  depends on  $\theta$ . Higher sensitivity is  
 188 observed for low than for high incidence angles (e.g., [43,44]). To include this dependence on  
 189 incidence angle, the soil moisture value is multiplied with the term  $\cotan(\theta)$ . Thus,  $g_{pq}(mv, \theta)$  can  
 190 be written as  $\delta 10^{\gamma \cotan(\theta) mv}$ .

191 The last term  $\Gamma_{pq}(kHrms, \theta)$  represents the behaviour of  $\sigma^{\circ}$  with soil roughness. An  
 192 exponential or logarithmic function is often used to express the radar signal (in dB) in terms of  
 193 surface roughness ([7,42,45-46]). For a logarithmic behaviour of  $\sigma^{\circ}$ (dB) with  $kHrms$ ,  $\Gamma_{pq}$  in linear  
 194 scale can be written as  $\mu(kHrms)^{\xi}$ . Baghdadi et al. [22] showed that at high incidence angles, radar  
 195 return is highly sensitive to surface roughness and shows much larger dynamics than at a low  
 196 incidence angle. In addition, the term  $\sin(\theta)$  is intended to include this dependence with the  
 197 incidence angle:  $\Gamma_{pq} = \mu(kHrms)^{\xi \sin(\theta)}$ .

198 Finally, the relationship between the radar backscattering coefficient ( $\sigma^{\circ}$ ) and the soil  
 199 parameters (soil moisture and surface roughness) for bare soil surfaces can be written by equation  
 200 (4):

$$\sigma_{pq}^{\circ} = \delta(\cos \theta)^{\beta} 10^{\gamma \cotan(\theta) mv} (kHrms)^{\xi \sin(\theta)} \quad (4)$$

201 The coefficients  $\delta$ ,  $\beta$ ,  $\gamma$ , and  $\xi$  are then estimated for each radar polarization using the method of  
 202 least squares by minimizing the sum of squares of the differences between the measured and  
 203 modelled radar signal. The error in the modelling of radar backscatter coefficients by the new  
 204 backscattering model was assessed for each polarization using a 5-fold cross-validation to validate  
 205 the predictive performance of the new model. To do the 5-fold cross-validation, the dataset was first  
 206 randomly divided into 5 equal size subsets. Next, 4 of the subsets are used to train the new model  
 207 and one was retained to validate its predictive performance. The cross-validation process was then  
 208 repeated 5 times, with each of the 5 sub-datasets used exactly once as the validation data. The final  
 209 validation result combines the 5 validation results. The advantage of this method over repeated  
 210 random sub-sampling is that all observations are used for both training and validation, and each  
 211 observation is used for validation exactly once.

212 The fitting of various coefficients parameter in the equation (4) was done using all dataset  
 213 (fitting errors are about 2 dB for all polarizations). This fitting allows writing  $\sigma^{\circ}$  as a function of the  
 214 rms surface height ( $Hrms$ ) and incidence angle ( $\theta$ ), by equations (5), (6) and (7):

$$\sigma_{HH}^{\circ} = 10^{-1.287} (\cos \theta)^{1.227} 10^{0.009 \cotan(\theta) mv} (kHrms)^{0.86 \sin(\theta)}, \quad (5)$$

$$\sigma_{VV}^{\circ} = 10^{-1.138} (\cos \theta)^{1.528} 10^{0.008 \cotan(\theta) mv} (kHrms)^{0.71 \sin(\theta)} \quad (6)$$

$$\sigma_{HV}^{\circ} = 10^{-2.325} (\cos \theta)^{-0.01} 10^{0.011 \cotan(\theta) mv} (kHrms)^{0.44 \sin(\theta)}, \quad (7)$$

215 where  $\theta$  is expressed in radians and  $mv$  is in vol.%. Equations (5), (6), and (7) show that the  
 216 sensitivity ( $\gamma$ ) of the radar signal to the soil moisture in decibel scale is 0.25 dB/vol.% in HH  
 217 polarization, 0.22 dB/vol.% in VV polarization and 0.30 dB/vol.% in HV polarization for an incidence

218 angle of 20°. This sensitivity decreases to 0.09 dB/vol.% in HH, 0.08 dB/vol.% in VV and 0.11  
 219 dB/vol.% for an incidence angle of 45°. As for the signal's sensitivity to soil roughness, it is of the  
 220 same order of magnitude in HH and VV and twice as large than that of the HV signal. The  
 221 availability of a backscatter model for the cross polarization component is required because the most  
 222 of spaceborne SAR acquisitions are made with one co-polarization and one cross-polarization in case  
 223 of dual-polarization mode.

#### 224 4.2. Results and discussion

##### 225 4.2.1. Performance of the new model

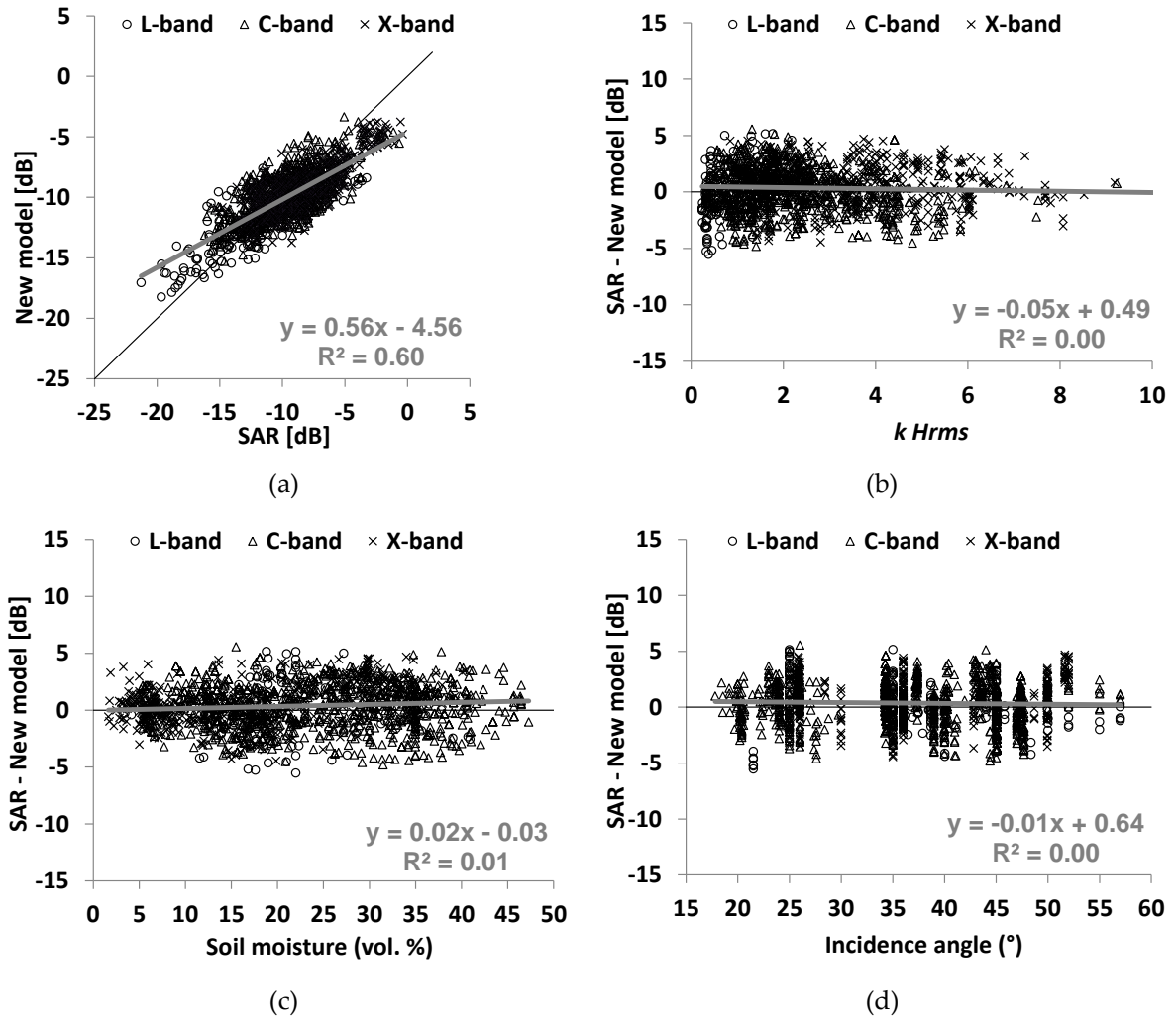
226 Results show that the new model provides more accurate results. The biases and the RMSE  
 227 decrease for both HH and VV polarizations. The RMSE decreases from 3.8 dB to 2.0 dB for HH and  
 228 from 2.8 dB to 1.9 dB for VV (Table 3). In addition, the high over- or underestimations of radar  
 229 backscattering coefficients observed with the Dubois model according to soil moisture, surface  
 230 roughness and radar incidence angle are clearly eliminated with the new model (Figures 3 and 4).

231 Analysis of the new model's performance for each radar wavelength separately (L-, C- and  
 232 X-bands) shows that the most significant improvement is observed in X-band with an RMSE that  
 233 decreases from 4.1 dB to 1.9 dB in HH and from 3.2 dB to 1.8 dB in VV. In L-band, the performance of  
 234 the new model is not better than that of the Dubois model because the RMSE decreases slightly with  
 235 the new model of 3.0 dB to 2.3 dB in HH and remains similar in VV (RMSE = 2.3 dB with the Dubois  
 236 model and 2.7 dB with the new model). The improvement is also important for the C-band with an  
 237 RMSE that decreases from 3.7 dB to 1.9 dB in HH and from 2.6 dB to 1.9 dB in VV. With respect to  
 238 bias, the results show that it decreases with the new model for all radar wavelengths. In addition, the  
 239 new model does not show bias according the range of soil moisture, surface roughness, and radar  
 240 incidence angle.

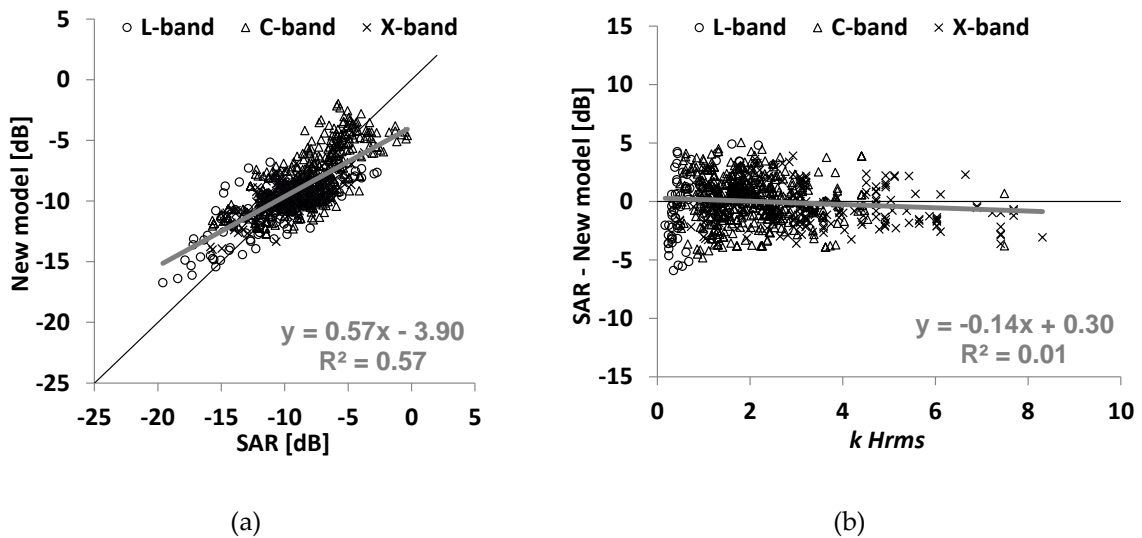
241 The comparison between the new model simulations in HV polarization (Equation 7) and the  
 242 real data (SAR data) shows an RMSE of 2.1 dB (Table 3) (1.6 dB in L-band, 2.2 dB in C-band, and 1.9  
 243 dB in X-band). The bias ( $\sigma^{\circ}$ SAR - model) is -1.3 dB in L-band, 0.2 dB in C-band, and -1.3 dB in  
 244 X-band. Figure 5 shows also that the new model correctly simulates the radar backscatter coefficient  
 245 in HV for all ranges of soil moisture, surface roughness and radar incidence angle.

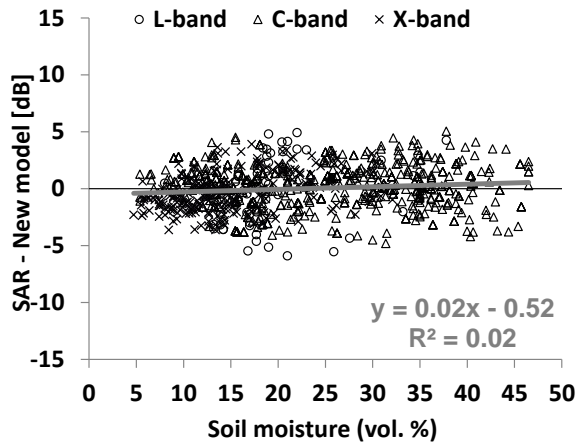
246 **Table 3.** Comparison between the results obtained with the Dubois model and those obtained with  
 247 the new model. Bias = real – model.

	Dubois for HH and VV		New model	
	Bias (dB)	RMSE (dB)	Bias (dB)	RMSE (dB)
<b>HH for all data</b>	-0.7	3.8	0.4	2.0
<b>VV for all data</b>	+0.9	2.8	0.0	1.9
<b>HV for all data</b>	-	-	0.0	2.1
<b>HH, L-band</b>	-0.8	2.9	-0.1	2.3
<b>HH, C-band</b>	-0.6	3.7	+0.3	1.9
<b>HH, X-band</b>	-0.7	4.1	0.7	1.9
<b>VV, L-band</b>	-0.2	2.3	-0.1	2.7
<b>VV, C-band</b>	+0.7	2.6	+0.1	1.9
<b>VV, X-band</b>	+2.0	3.2	-0.4	1.8
<b>HV, L-band</b>	-	-	-1.3	1.6
<b>HV, C-band</b>	-	-	+0.2	2.2
<b>HV, X-band</b>	-	-	-1.3	1.9

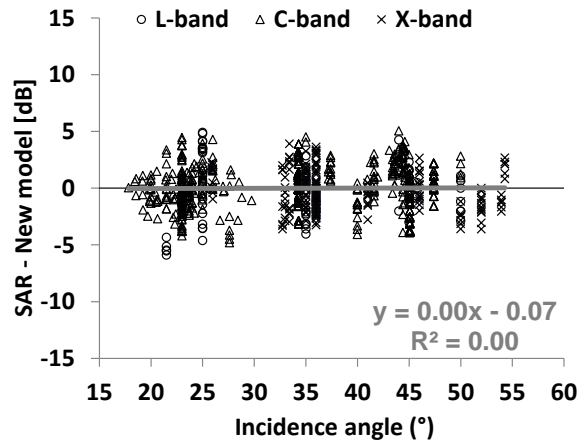


248 **Figure 3.** (a) Comparison between  $\sigma^0$  modelled in the new model and  $\sigma^0$  measured (for all SAR  
 249 bands) for HH polarization, (b) difference between SAR and the new model as a function of surface  
 250 roughness ( $kHrms$ ), (c) difference between SAR and the new model as a function of soil moisture  
 251 ( $mv$ ), (d) difference between SAR and the new model as a function of incidence angle. The best  
 252 regression model is plotted in gray.





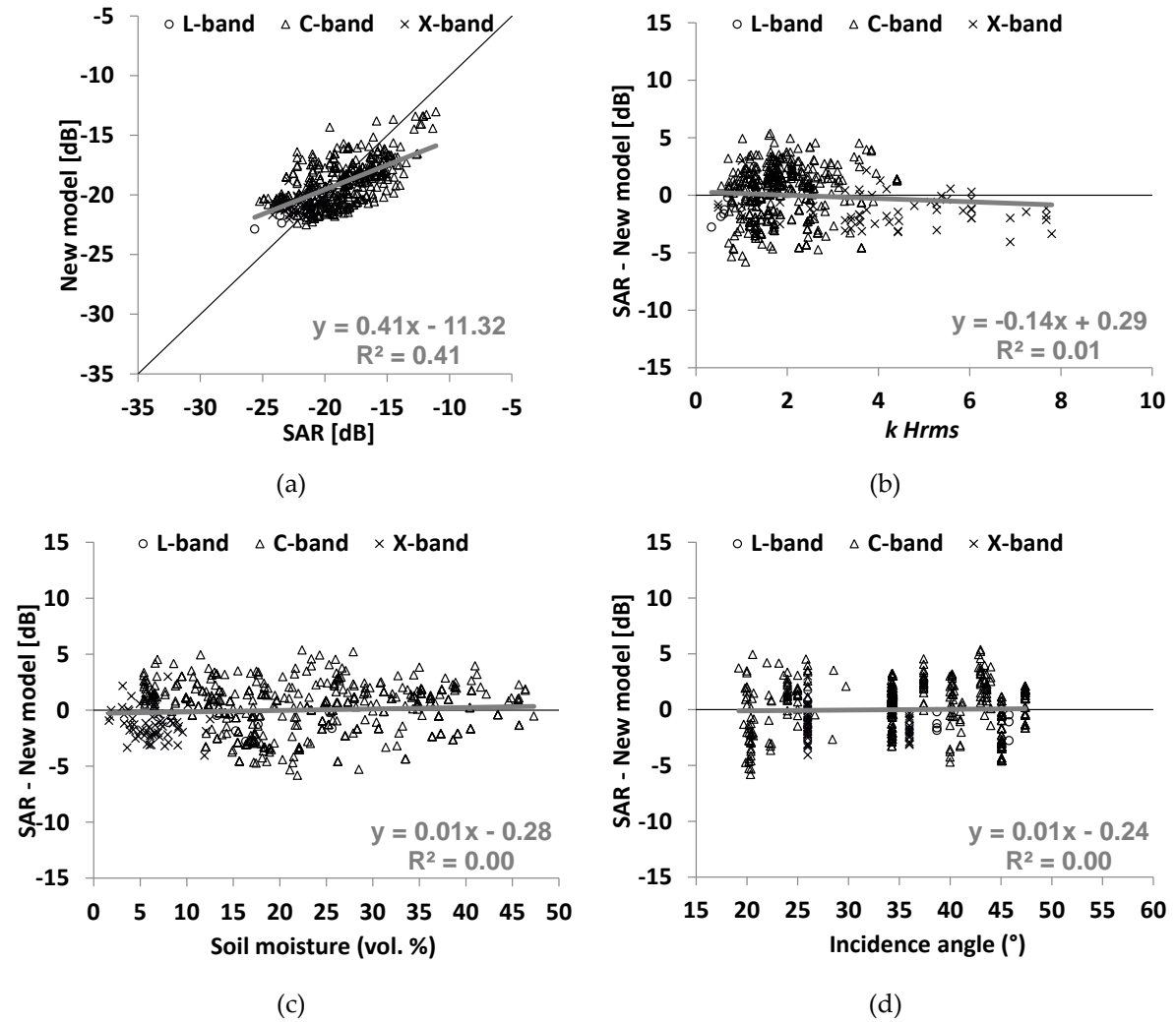
(c)



(d)

253 **Figure 4.** (a) Comparison between  $\sigma^o$  in the new model and  $\sigma^o$  measured (for all SAR bands) for VV  
 254 polarization, (b) difference between SAR and the new model as a function of surface roughness  
 255 ( $kHrms$ ), (c) difference between SAR and the new model as a function of soil moisture ( $mv$ ), (d)  
 256 difference between SAR and the new model as a function of incidence angle. The best regression  
 257 model is plotted in gray.

258



259 **Figure 5.** (a) Comparison between  $\sigma^{\circ}$  in the new model and  $\sigma^{\circ}$  measured (for all SAR bands) for HV  
 260 polarization, (b) difference between SAR and the new model as a function of  $kHrms$ , (c) difference  
 261 between SAR and the new model as a function of  $mv$ , (d) difference between SAR and the new model  
 262 as a function of incidence angle. The best regression model is plotted in gray.

263 4.2.2. Behaviour of the new model

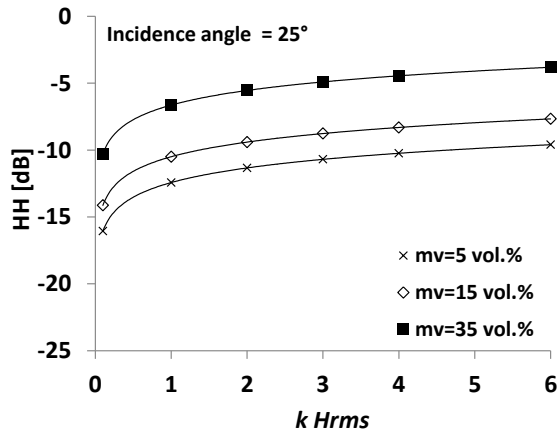
264 The physical behaviour of the new radar backscatter model was studied in function of incidence  
 265 angle ( $\theta$ ), soil moisture ( $mv$ ) and surface roughness ( $kHrms$ ).

266 Figure 6 shows that the radar signal is strongly sensitive to surface roughness, especially for  
 267 small values of  $kHrms$ . In addition, this sensitivity increases with the incidence angle. Concerning the  
 268 influence of polarization, the new model shows, as do many theories and experimental studies, that  
 269 a given soil roughness leads to slightly higher signal dynamics with the soil moisture in HH than in  
 270 VV polarization [17,47]. The radar signal  $\sigma^{\circ}$  increases with  $kHrms$ . This increase is higher for either  
 271 low  $kHrms$  values or high  $\theta$ -values than it is for either high  $kHrms$  values or low  $\theta$ -values. For  $\theta=45^{\circ}$ ,  
 272  $\sigma^{\circ}$  increases approximately 8 dB in HH and 6.5 dB in VV when  $kHrms$  increases from 0.1 to 2  
 273 compared with only 3 dB when  $kHrms$  increases from 2 to 6 (for both HH and VV). This dynamic of  
 274  $\sigma^{\circ}$  is only half for  $\theta=25^{\circ}$  in comparison to that for  $\theta=45^{\circ}$ . In HV, the dynamic of  $\sigma^{\circ}$  to  $kHrms$  is half  
 275 that observed for HH and VV.

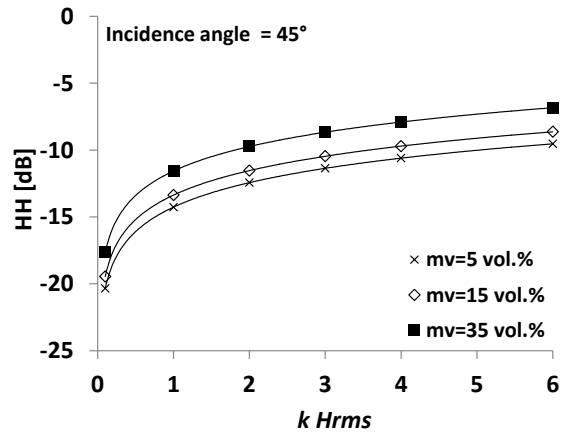
276 The behaviour of  $\sigma^{\circ}$  according to soil moisture shows a larger increase of  $\sigma^{\circ}$  with  $mv$  for low  
 277 incidence angles than for high incidence angles. Figure 6 shows that  $\sigma^{\circ}_{HH}$  and  $\sigma^{\circ}_{VV}$  increase  
 278 approximately 6 dB for  $\theta=25^{\circ}$  compared with only 3 dB for  $\theta=45^{\circ}$  when  $mv$  increases from 5 to 35

279 vol.%. In HV, the signal increases approximately 7.5 dB for  $\theta=25^\circ$  and 3.5 dB for  $\theta=45^\circ$  when  $mv$   
 280 increases from 5 to 35 vol.%.  
 281

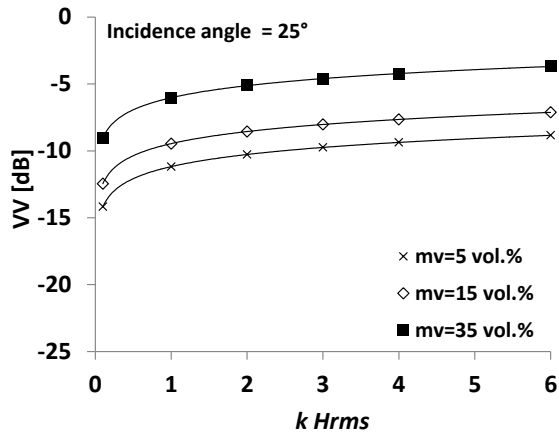
As mentioned in Dubois et al. [12], the ratio  $\frac{\sigma_{HH}^\circ}{\sigma_{VV}^\circ}$  should increase with  $kHrms$  and remain  
 282 less than 1. The new model shows that this condition is satisfied when  $20^\circ < \theta < 45^\circ$ ,  $kHrms < 6$  and  
 283  $mv < 35$  vol.%.



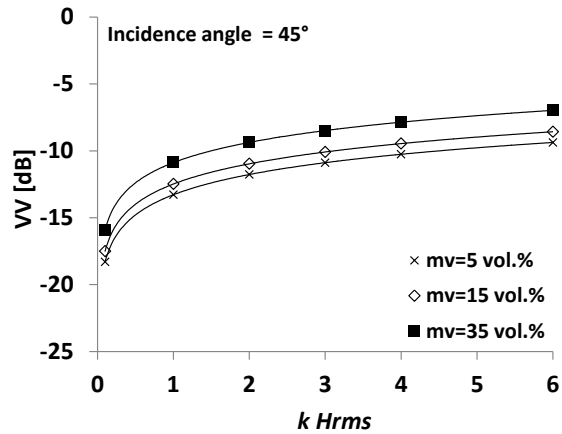
(a)



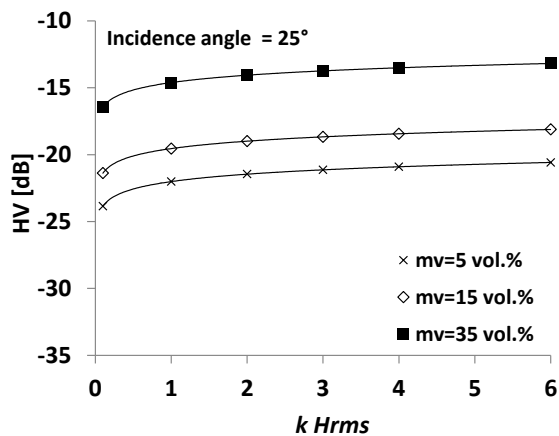
(b)



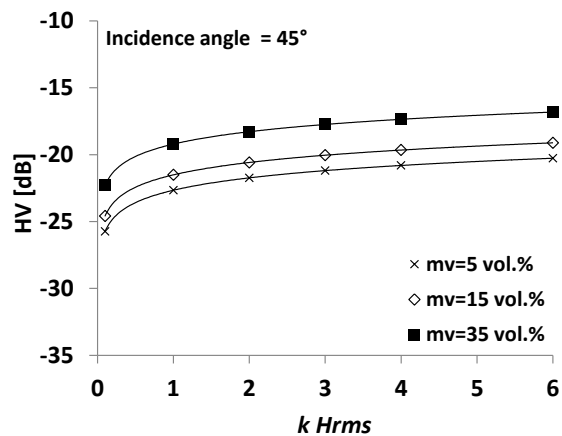
(c)



(d)



(e)



(f)

284 **Figure 6.** Behavior of the new model as a function of incidence angle, surface roughness ( $k$  Hrms) and  
 285 soil moisture ( $mv$ ) in HH, VV and HV polarizations.

## 286 5. Conclusion

287 This investigations objective is to propose a new empirical model for radar backscatter from  
 288 bare soil surfaces. The new model is based on the formulation made in the Dubois model where the  
 289 radar signal in HH and VV polarizations is described according to radar wavelength, incidence  
 290 angle, soil moisture and roughness. This new model is based on the formulation made in the Dubois  
 291 model. A large dataset was used, composed of ground measurements and SAR images over bare  
 292 agricultural soils.

293 Results show that the new model provides improved results in comparison to the Dubois  
 294 model (in the case of HH and VV). Biases and RMSE have decreased for both HH and VV  
 295 polarizations. In addition, the high over- or under-estimations observed with the Dubois model for  
 296 some ranges of soil moisture, surface roughness and radar incidence angle were clearly eliminated  
 297 with the new model. Analysis of the new model's performance for each radar wavelength separately  
 298 (L, C and X) shows that in the L-band, the performance of the new model was similar to that of the  
 299 Dubois model. The model shows significant improvement in C- and X-bands (RMSE approximately  
 300 1.9 dB with the new model and between 2.6 and 4.1 dB with the Dubois model).

301 Based on the same equation as that used for HH and VV, a radar signal in HV polarization was  
 302 also proposed. Finally, the new empirical model proposed in the present study would allows more  
 303 accurate soil moisture estimates using the new Sentinel-1A and -1B SAR data.

304 **Acknowledgements:** This research was supported by IRSTEA (National Research Institute of Science  
 305 and Technology for Environment and Agriculture), the French Space Study Center (CNES, TOSCA 2016) and  
 306 the Belgian Science Policy Office (Contract SR/00/302). H. Lievens is a postdoctoral research fellow of the  
 307 Research Foundation Flanders (FWO). Authors thank the space agencies that provided AIRSAR, SIR-C, JERS-1,  
 308 ERS-1/2, RADARSAT-1/2, ASAR, PALSAR-1, TerraSAR-X, COSMO-SkyMed, and ESAR data.

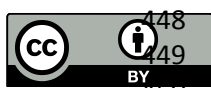
## 309 References

- 310 1. Rao, S.S.; Kumar, S.D.; Das, S.N. Modified dubois model for estimating soil moisture with dual  
 311 polarized SAR data. *J. Indian Soc. Remote Sensing*, **41**, p. 865–872, 2013.
- 312 2. Chai, X.; Zhang, T.T.; Shao, Y.; Gong, H.Z.; Liu, L.; Xie, K.X. Modeling and mapping soil  
 313 moisture of plateau pasture using RADARSAT-2 imagery. *Remote Sensing*, **7**, p. 1279–1299,  
 314 2015.
- 315 3. Kirimi F., Kuria D.N., Frank Thonfeld F., Amler E., Mubea K., Misana S., Gunter Menz G., 2016.  
 316 Influence of Vegetation Cover on the Oh Soil Moisture Retrieval Model: A Case Study of the  
 317 Malinda Wetland, Tanzania. *Advances in Remote Sensing*, **5**, p. 28-42, 2016.
- 318 4. Gherboudj I., Magagi R., Berg A.A., Toth B., Soil moisture retrieval over agricultural fields from  
 319 multi-polarized and multi-angular RADARSAT-2 SAR data. *Remote Sensing of Environment*,  
 320 **115**, p. 33-43, 2011.
- 321 5. Zribi M., Chahbi A., Shabou M., Lili-Chabaane Z., Duchemin B., Baghdadi N., Amri R.,  
 322 Chehbouni A., Soil surface moisture estimation over a semi-arid region using ENVISAT ASAR  
 323 radar data for soil evaporation evaluation. *Hydrology and Earth System Sciences*, **15**, p.  
 324 345-358, 2011.
- 325 6. Le Hegarat-Masclé S., Zribi M., Alem F., Weisse A., Loumagne C., Soil moisture estimation  
 326 from ERS/SAR data: Toward an operational methodology. *IEEE Transactions on Geoscience  
 327 and Remote Sensing* **40/12**, p. 2647-2658, 2002.
- 328 7. Zribi M., Dechambre M., A new empirical model to retrieve soil moisture and roughness from  
 329 Radar Data. *Remote Sensing of Environment*, **84/1**, p. 42-52, 2003.
- 330 8. Oh Y., Sarabandi K., Ulaby F.T., An empirical model and an inversion technique for radar  
 331 scattering from bare soil surfaces. *IEEE Transactions on Geoscience and Remote Sensing*, **30(2)**,  
 332 p. 370-381, 1992.

- 333 9. Oh Y., Kay Y., Condition for precise measurement of soil surface roughness. *IEEE Transactions on Geoscience and Remote Sensing*, 36(2), p. 691-695, 1998.
- 334
- 335 10. Oh Y., Sarabandi K., Ulaby F.T., Semi-empirical model of the ensemble-averaged differential  
336 Mueller matrix for microwave backscattering from bare soil surfaces. *IEEE Transactions on*  
337 *Geoscience and Remote Sensing*, 40, p. 1348-1355, 2002.
- 338 11. Oh Y., Quantitative retrieval of soil moisture content and surface roughness from  
339 multipolarized radar observations of bare soil surfaces. *IEEE Transactions on Geoscience and*  
340 *Remote Sensing*, 42, p. 596-601, 2004.
- 341 12. Dubois P.C., Van Zyl J., Engman T., Measuring soil moisture with imaging radars. *IEEE*  
342 *Transactions on Geoscience and Remote Sensing*, 33, p. 915-926, 1995.
- 343 13. Baghdadi N., Saba E., Aubert M., Zribi M., Baup F., Comparison between backscattered  
344 TerraSAR signals and simulations from the radar backscattering models IEM, Oh, and Dubois.  
345 *IEEE Geosci. Remote Sens. Lett.* 8, p. 1160-1164, 2011.
- 346 14. Baghdadi N., Zribi M., Evaluation of radar backscatter models IEM, Oh and Dubois using  
347 experimental observations. *Int. J. Remote Sens.*, 27, p. 3831-3852, 2006.
- 348 15. Wang H., Méric S., Allain S., and Pottier E., Adaptation of Oh Model for Soil Parameters  
349 Retrieval Using Multi-Angular RADARSAT-2 Datasets. *Journal of Surveying and Mapping*  
350 *Engineering*, 2(4), p. 65-74, 2014.
- 351 16. Wang J.R., Hsu A., Shi J.C., O'Neill P.E., Engman E.T., A comparison of soil moisture retrieval  
352 models using SIR-C measurements over the Little Washita River watershed». *Remote Sensing*  
353 *Environment*, 59, p. 308-320, 1997.
- 354 17. Zribi M., Taconet O., Le Hégarat-Masclé S., Vidal-Madjar D., Emblanch C., Loumagne C.,  
355 Normand M., Backscattering behavior and simulation comparison over bare soils using  
356 SIRC/XSAR and ERASME 1994 data over Orgeval. *Remote Sensing of Environment*, 59(2), p.  
357 256-266, 1997.
- 358 18. Baghdadi N., Dubois-Fernandez P., Dupuis X., Zribi M., Sensitivity of multi polarimetric  
359 parameters of multifrequency polarimetric SAR data to soil moisture and surface roughness  
360 over bare agricultural soils. *IEEE Geoscience and Remote Sensing Letters*, 10(4), p. 731-735,  
361 2013.
- 362 19. Baghdadi N., Zribi M., Loumagne C., Ansart P., Paris Anguela T., Analysis of TerraSAR-X data  
363 and their sensitivity to soil surface parameters over bare agricultural fields. *Remote Sensing of*  
364 *Environment*, 112(12), p. 4370-4379, 2008.
- 365 20. Baghdadi N., Aubert M., Zribi M., Use of TerraSAR-X data to retrieve soil moisture over bare  
366 soil agricultural fields. *IEEE Geoscience and Remote Sensing Letters*, 9(3), p. 512-516, 2012.
- 367 21. Baghdadi N., Gherboudj I., Zribi M., Sahebi M., Bonn F., King C., Semi-empirical calibration of  
368 the IEM backscattering model using radar images and moisture and roughness field  
369 measurements. *International Journal of Remote Sensing*, 25(18), p. 3593-3623, 2004.
- 370 22. Baghdadi N., King C., Bourguignon A., Remond A., Potential of ERS and RADARSAT data for  
371 surface roughness monitoring over bare agricultural fields: application to catchments in  
372 Northern France. *International Journal of Remote Sensing*, 23(17), p. 3427-3442, 2002.
- 373 23. Holah H., Baghdadi N., Zribi M., Bruand A., King C., Potential of ASAR/ENVISAT for the  
374 characterisation of soil surface parameters over bare agricultural fields. *Remote Sensing of*  
375 *Environment*, 96(1), p. 78-86, 2005.
- 376 24. Baghdadi N., Holah N., Zribi M., Calibration of the Integral Equation Model for SAR data in  
377 C-band and HH and VV polarizations. *International Journal of Remote Sensing*, 27(4), p.  
378 805-816, 2006.
- 379 25. Le Morvan A., Zribi M., Baghdadi N., and Chanzy A., Soil moisture profile effect on radar  
380 signal measurement. *Remote Sensing*, 8, p. 256-270, 2008.
- 381 26. Baghdadi N., Saba E., Aubert M., Zribi M., Baup F., Comparison between backscattered  
382 TerraSAR signals and simulations from the radar backscattering models IEM, Oh, and Dubois,  
383 *IEEE Geoscience and Remote Sensing Letters*, 8(6), p.1160-1164, doi:  
384 10.1109/LGRS.2011.2158982, 2011.

- 385 27. Baghdadi N., Cresson R., El Hajj M., Ludwig R., La Jeunesse I., Estimation of soil parameters  
386 over bare agriculture areas from C-band polarimetric SAR data using neural networks.  
387 Hydrology and Earth System Sciences (HESS), 16, p. 1607-1621, doi:10.5194/hess-16-1607-2012,  
388 2012.
- 389 28. Baghdadi N., Aubert M., Cerdan O., Franchistéguy L., Viel C., Martin E., Zribi M., Desprats J.F.,  
390 Operational mapping of soil moisture using synthetic aperture radar data: application to Touch  
391 basin (France). Sensors Journal, 7, p. 2458-2483, 2007.
- 392 29. Zribi M., Gorrab A., Baghdadi N., Lili-Chabaane Z., Influence of radar frequency on the  
393 relationship between bare surface soil moisture vertical profile and radar backscatter, IEEE  
394 Geoscience and Remote Sensing Letters, 11(4), p. 848-852, doi: 10.1109/LGRS.2013.2279893,  
395 2014.
- 396 30. Gorrab A., Zribi M., Baghdadi N., Mougénot B., Lili-Chabaane Z., Retrieval of both soil  
397 moisture and texture using TerraSAR-X images, Remote Sensing, 7, p. 10098-10116,  
398 doi:10.3390/rs70810098, 2015.
- 399 31. Aubert M., Baghdadi N., Zribi M., Ose K., El Hajj M., Vaudour E., Gonzalez-Sosa E., Toward an  
400 operational bare soil moisture mapping using TerraSAR-X data acquired over agricultural  
401 areas, IEEE Journal of Selected Topics in Applied Earth Observations and Remote Sensing  
402 (JSTARS), 6(2), p. 900-916, doi: 10.1109/JSTARS.2012.2220124, 2013.
- 403 32. Dong L., Baghdadi N., Ludwig R., Retrieving surface soil moisture using radar imagery in a  
404 semi-arid environment. IEEE Geoscience and Remote Sensing Letters, 10(3), p. 461-465, 2013.
- 405 33. Baup F., Fieuzal R., Marais-Sicre C., Dejoux J-F., le Dantec V., Mordelet P., Claverie M., Hagolle  
406 O., Lopes A., Keravec P., Ceschia E., Mialon A., Kidd R., MCM'10: An experiment for satellite  
407 multi-sensors crop monitoring. From high to low resolution observations, Geoscience and  
408 Remote Sensing Symposium, p. 4849-4852, 2012.
- 409 34. Mattia M., Toan T.L., Souyris J.C., Carolis G.D., Floury N., Posa F., Pasquariello G., The effect of  
410 surface roughness on multifrequency polarimetric SAR data. IEEE Trans. Geosci. Remote Sens.,  
411 35(4), p. 954-966, 1997.
- 412 35. Lievens H., Verhoest N.E.C., De Keyser E., Vernieuwe H., Matgen P., Álvarez-Mozos J.,  
413 De Baets B., Effective roughness modelling as a tool for soil moisture retrieval from C-and  
414 L-band SAR, Hydrology and Earth System Sciences, 15(1), p. 151-162, 2011.
- 415 36. Baronti S., Del Frate F., Ferrazzoli P., Paloscia S., Pampaloni P., Schiavon G., SAR polarimetric  
416 features of agricultural areas, International Journal of Remote Sensing, 16(14), p. 2639-2656,  
417 1995.
- 418 37. Macelloni G., Paloscia S., Pampaloni P., Sigismondi S., de Matthæis P., Ferrazzoli P., Schiavon  
419 G., Solimini D., The SIR-C/X-SAR experiment on Montespertoli: sensitivity to hydrological  
420 parameters, International Journal of Remote Sensing, 1999, 20(13), p. 2597-2612, 1999.
- 421 38. Paloscia S., Macelloni G., Pampaloni P., Sigismondi S., The potential of C- and L-band SAR in  
422 estimating vegetation biomass: the ERS-1 and JERS-1 Experiments, IEEE Trans.on Geosci. and  
423 Remote Sensing, 37(3), p. 2107-2110, 1999.
- 424 39. Ulaby F.T., Moore R.K., Fung A.K., Microwave Remote Sensing, vol. II (New York:  
425 Addison-Wesley), 1982.
- 426 40. Beauchemin M., Thomson K., Edwards G., Modelling forest stands with MIMICS: implications  
427 for calibration. Canadian Journal of Remote Sensing, 21, p. 518-526, 1995.
- 428 41. Baghdadi N., Bernier M., Gauthier R., Neeson I., Evaluation of C-band SAR data for wetlands  
429 mapping. International Journal of Remote Sensing, 22, p. 71-88, 2001.
- 430 42. Baghdadi N., Holah N., Zribi M., Soil moisture estimation using multi-incidence and  
431 multi-polarization ASAR SAR data. In: International Journal of Remote sensing, 27/10, p.  
432 1907-1920, 2006.
- 433 43. Aubert M., Baghdadi N., Zribi M., Douaoui A., Loumagne C., Baup F., El Hajj M., Garrigues S.,  
434 Characterization of soil surface by TerraSAR-X imagery. Remote Sensing of Environment, 115,  
435 p. 1801-1810, 2011.

- 436 44. Baghdadi N., Cerdan O., Zribi M., Auzet V., Darboux F., El Hajj M., Bou Kheir R., Operational  
437 performance of current synthetic aperture radar sensors in mapping soil surface characteristics  
438 in agricultural environments: application to hydrological and erosion modelling. *Hydrological*  
439 *Processes*, 22, p. 9-20, 2008.
- 440 45. Srivastava H.S., Patel P., Manchanda M.L., Adiga S., Use of multi-incidence angle  
441 RADARSAT-1 SAR data to incorporate the effects of surface roughness in soil moisture  
442 estimation. *IEEE Transactions on Geosciences and Remote Sensing*, 41, p. 1638-1640, 2003.
- 443 46. Sahebi M.R., Angles J., Bonn F., A comparison of multi-polarization and multi-angular  
444 approaches for estimating bare soil surface roughness from spaceborne radar data. *Canadian*  
445 *Journal of Remote Sensing*, 28(5), p. 641-652, 2002.
- 446 47. Fung A. K., 1994. *Microwave Scattering and Emission Models and their Applications*. Artech  
447 House, Inc., Boston, London, 573 pages.



© 2016 by the authors. Submitted for possible open access publication under the terms and conditions of the Creative Commons Attribution (CC-BY) license (<http://creativecommons.org/licenses/by/4.0/>).